Available online at www.sciencedirect.com
ScienceDirect
Trans. Nonferrous Met. Soc. China 25(2015) 261−270
Transactions of Nonferrous Metals Society of China
www.tnmsc.cn

Finite element analysis of stress distribution and burst failure of SiC_f/Ti−6Al−4V composite ring

Hong-yuan ZHANG, Yan-qing YANG, Xian LUO

State Key Laboratory of Solidification Processing, School of Materials Science and Engineering, Northwestern Polytechnical University, Xi'an 710072, China

Received 7 December 2013; accepted 23 September 2014

Abstract: A three-dimensional cyclic symmetry finite element model of titanium-matrix composites (TMCs) ring was developed to investigate the stress distribution and burst failure. The effects of fiber volume fractions, reinforced areas, thermal residual stresses and two different temperatures on stress distribution were studied. The burst speed was obtained through analyzing the hoop tensile stresses under a series of rotating speeds. The results indicate that at the two different temperatures, the influences of fiber volume fractions and reinforced areas on stress level and distribution are different. Some proposals are provided for the structure design of the TMCs ring. With regard to thermal residual stresses, a larger reinforced area is an advisable choice for design of the ring at higher temperature.

Key words: titanium-matrix composites; ring; stress distribution; burst failure; finite element analysis; thermal residual stresses

1 Introduction

In advanced engine designs, light-weight materials are desirable that allow higher operating speeds and longer durability [1]. This is particularly the case of continuous SiC fiber reinforced titanium-matrix composites (TMCs) owing to their excellent performances along the fiber direction, such as high specific strength, stiffness and high creep resistance [2]. One potential application of TMCs is integrally bladed compressor rings in aeroengine gas turbines, with potential weight saving up to 50% as compared with the conventional disc and blades assembly [3]. For this new design, the availability of TMCs appears to be a prerequisite since monolithic titanium alloys will not be capable of withstanding the loads imposed on the rings during service.

For advanced turbine engine designs, to realize the potential benefits offered by TMCs, several key issues, such as component design, fabrication, inspection and analysis method of structural behavior must be developed and demonstrated due to anisotropic properties and different failure mode of TMCs in comparison with traditional metal materials. Static burst failure and fatigue life in a cyclic loading condition are basic key issues from the point of reliability. Realizing the significance of this point, ARNOLD and WILT [4] modeled static burst and cyclic fatigue lives of subscale TMCs reinforced rings representative of those used in advanced compressor rotor designs through a nonlinear finite element code MARC. In their work, a uniform pressure was applied to the inside diameter surface of the ring to induce radial compressive and hoop tensile stresses. They obtained a limit pressure of 221 MPa on the basis of strain-to-failure criterion at 427 °C, and predicted that the damage would initiate along the inner diameter of the composite core. ROBINSON and PASTOR [5] calculated the limit loads of SiC_f/Ti composites ring subjected to interior pressure by using an anisotropic perfect plasticity theory and gave an estimated failure pressure range of 172−200 MPa at 427 °C. However, in the above mentioned studies, interior pressure was applied to induce hoop tensile stresses. In reality, the ring should rotate when working, and hoop tensile stresses would be generated due to the centrifugal forces. NATSUMURA et al [6] conducted numerical analysis and spin test to investigate the failure

Foundation item: Projects (51071122, 51271147, 51201134) supported by the National Natural Science Foundation of China; Project (3102014JCQ01023) supported by the Fundamental Research Funds for the Central Universities; Project (115-QP-2014) supported by the Research Fund of the State Key Laboratory of Solidification Processing in Northwestern Polytechnical University, China
Corresponding author: Yan-qing YANG; Tel/Fax: +86-29-88460499; E-mail: yqyang@nwpu.edu.cn
DOI: 10.1016/S1003-6326(15)63601-9

mode and mechanism of TMCs ring. It was found that the primary failure was caused by tensile overload in the hoop direction. KRUCH et al [7] constructed a macroscopic model based on micromechanics, coupling viscoplasticity, damage and thermal effects to perform the fatigue analysis of bladed ring (bling) by using a finite element code Zebulon. The results showed that the weakest zone was located close to the inner diameter of the reinforced zone during high cycle fatigue.

Nevertheless, literatures investigating the stress distribution of a large size of structural component made of TMCs applied to compressor rotors are limited, and previous studies concerning TMCs mostly focus on interfacial reactions, mechanical properties and micro finite element modeling. In this work, a 3D cyclic symmetry finite element model is constructed to simulate the stress distribution of TMCs ring with and without consideration of thermal residual stresses at room temperature and 400 °C, respectively. The attention is focused on investigating the influence of fiber volume fractions and reinforced areas on hoop stresses. Then a "maximum hoop stress" criterion is used to predict the burst speed.

2 Finite element analysis

2.1 3D finite element model

The finite element analysis is implemented through ANSYS code. As shown in Fig. 1, a 3D cyclic symmetry finite element model of 1/20 of the ring consisting of SiC_f/Ti−6Al−4V composite core and matrix cladding is constructed. The inner diameter (ID) and outer diameter (OD) of the TMC rings are 400 mm and 500 mm, respectively, with an axial height of 40 mm. The boundary conditions are set as follows: three selected nodes at x=200 and z=0 whose y coordinate is respectively y=0°, y=9° and y=18° are not allowed to move in z-direction, at the same time, all the nodes mentioned above are also not allowed to move in y-direction to prevent rigid body displacement; all the corresponding nodes at the two cyclic symmetry planes (i.e., the planes at y=0° and y=18°) have an equal displacement in x, y and z directions. The coordinate system mentioned above is a global cylindrical system. Three dimensional elements SOLID45 and SOLID186 are selected for the matrix cladding and the composite core, respectively.

To study the influence of fiber volume fractions on stress distribution of the TMC rings, composite core with fiber volume fractions of 30%, 35% and 40% are investigated when reinforced area is 30 mm×20 mm in cross section shown in Fig. 1(b). For different reinforced areas, as the fiber volume fraction is controlled to be 35%, the reinforced areas are 30 mm×20 mm, 30 mm×30 mm and 40 mm×30 mm in the middle of the cross section, respectively.

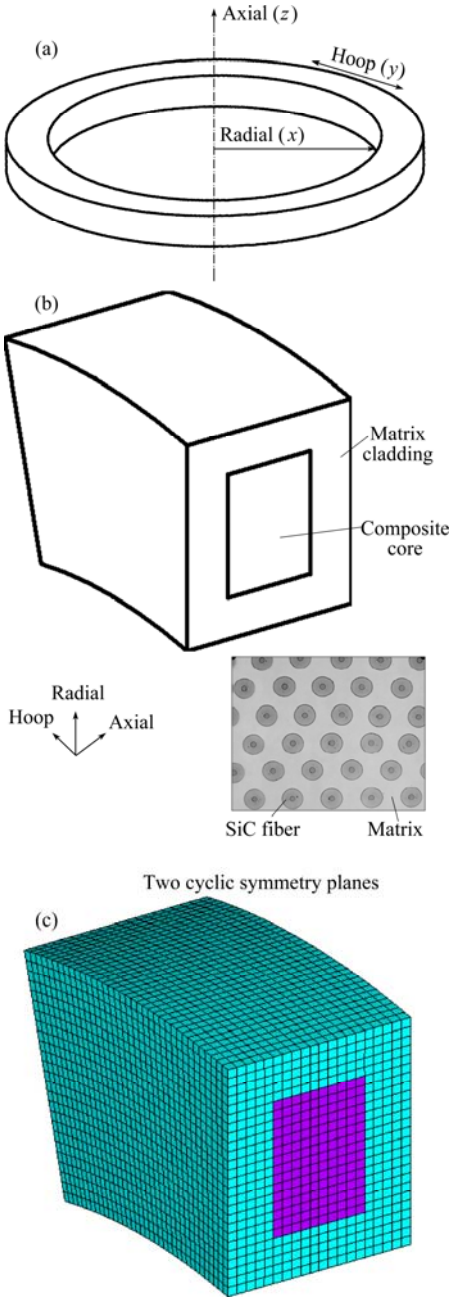

Fig. 1 Finite element model of TMC rings: (a) Whole TMCs ring; (b) 1/20 of TMCs ring; (c) Finite element model

2.2 Properties of constituents

The matrix cladding is considered to be isotropic elastic-plastic behavior (see Table 1). The plasticity is introduced by the von Mises yield criterion. The composite core is assumed to be a transversely isotropic material described by Hill's anisotropic elastic-plastic constitutive model [8]. As the transversely isotropic material is a special case of orthotropic, there are five dependent elastic parameters. Due to the limited

experimental data on temperature-dependent mechanical properties and coefficients of thermal expansion (CTEs) of composites along and transverse to fiber direction, Whitney-Riley model [9] is used to predict the elastic constants of the composites, which has been proved to agree well with available experiment data. The CTEs of the composites in longitudinal direction are predicted by Schapery's model [10]. However, the CTEs of composites in transverse direction are calculated by "Local Role of Mixture" [11]. The ultimate tensile strength in longitudinal direction of the composite with 35% fiber volume fraction predicted by modified role of mixture [12] is 1412 MPa at room temperature, while the value reduces to 1162 MPa at 400 °C mainly because of the matrix softening. The associated material parameters with 35% fiber volume fraction are given in Table 2. It is assumed that the longitudinal response is pure elastic until failure (i.e., ε_f=0.0068 and σ_u=1412 MPa). It should be pointed out that the parameters of the composites with other fiber volume fractions are also obtained with the same method.

2.3 Finite element analysis

The analytical procedure contains two steps. The first is modeling the thermal residual stresses between matrix cladding and composite core, and the second is modeling the centrifugal forces under certain angular velocity. The composite core is assumed to be perfectly bonded with the matrix cladding during the processing of hot iso-static pressure (HIP). For the stress analysis, burst speed prediction, initial damage due to fabrication, such as micro-cracks, are not included. Thermal residual stresses are induced when TMCs ring is cooled from consolidation temperature to service temperature owing to mismatch of the CTEs between the composite core and the matrix cladding. The cooling process is modeled by imposing thermal loading. The reference temperature is assumed to be 700 °C [4] above which the composite core and matrix cladding are stress free.

3 Results and discussion

3.1 Model verification

In the finite element analysis for stress distribution of TMCs ring, in order to assess the correctness of the model, an analytical method [15] was used to calculate the distribution of hoop stresses as well as radial stresses for a solid composite and a solid matrix ring at a rotating speed of 14320 r/min at room temperature, respectively. The fiber volume fraction for the solid composite ring is 35%. Clearly, in such cases, no CTEs mismatch between composite core and matrix cladding, thus no residual stresses was observed. The stress distributions for the solid composite and solid matrix ring are shown in Fig. 2 and Fig. 3, respectively. As it can be seen, hoop stresses and radial stresses calculated through the analytical method are in excellent agreement with those of finite element simulation, which confirms the correctness of the finite element model. In addition, both the results show that hoop stresses have a maximum value at the ID of the ring and then gradually reduce along the radial direction, while the radial stresses have a maximum

Table 1 Properties of Ti−6Al−4V matrix at different temperatures [13,14]

Temperature/ °C	Elastic modulus, E/GPa	Yield strength, σ_y/MPa	Hardening modulus, H/GPa	Coefficient of thermal expansion, α/(10^{-6} °C^{-1})	Poisson ratio, v	Density, ρ/(kg·m^{-3})
23	105.0	890.9	0.53	8.8	0.23	4440
200	94.7	690.9	0.67	9.4	0.23	4440
400	84.1	563.6	0.69	10.3	0.23	4440
600	74.2	381.8	0.21	10.8	0.23	4440
800	62.8	218.2	0.13	11.5	0.23	4440

Table 2 Properties of SiC_f/Ti−6Al−4V composites at different temperatures

Temperature/ °C	Elastic modulus, E/GPa		Poisson ratio, v		Shear modulus, G/GPa		Coefficient of thermal expansion, α/(10^{-6} °C^{-1})		Longitudinal yield strength, σ_{uL}/MPa	Density, ρ/(kg·m^{-3})
	L	T	L	T	L	T	L	T		
23 °C	209.0	157.1	0.237	0.2385	64.4	63.4	5.57	6.64	1412	3778.5
200 °C	202.3	145.1	0.237	0.2385	59.6	58.6	5.64	7.03		3778.5
400 °C	195.4	132.3	0.237	0.2386	54.3	53.4	5.76	7.62	1162	3778.5
600 °C	188.9	119.8	0.237	0.2386	49.2	48.4	5.73	7.94		3778.5
800 °C	181.5	104.6	0.237	0.2387	42.9	42.2	5.68	8.40		3778.5

L: Longitudinal; T: Transverse.

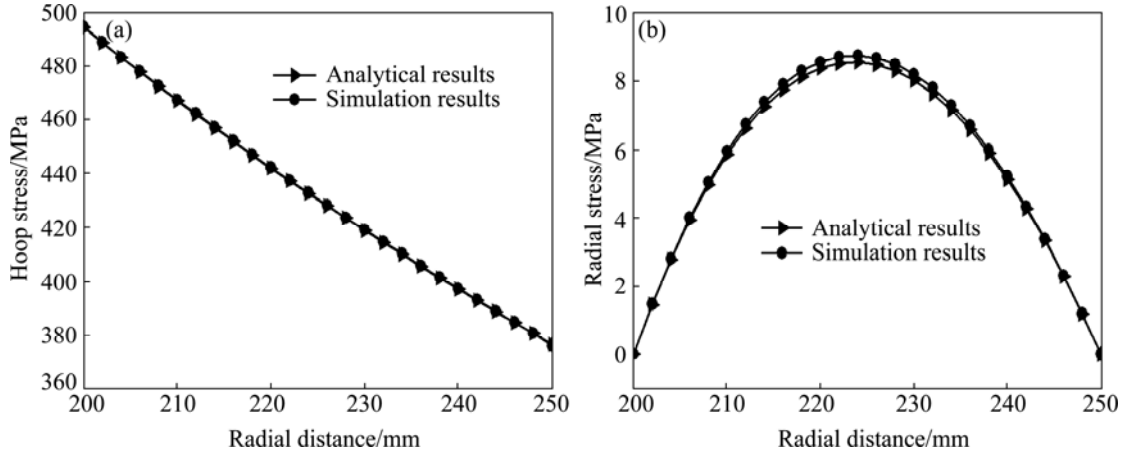

Fig. 2 Stress distributions of solid composite ring: (a) Hoop stress; (b) Radial stress

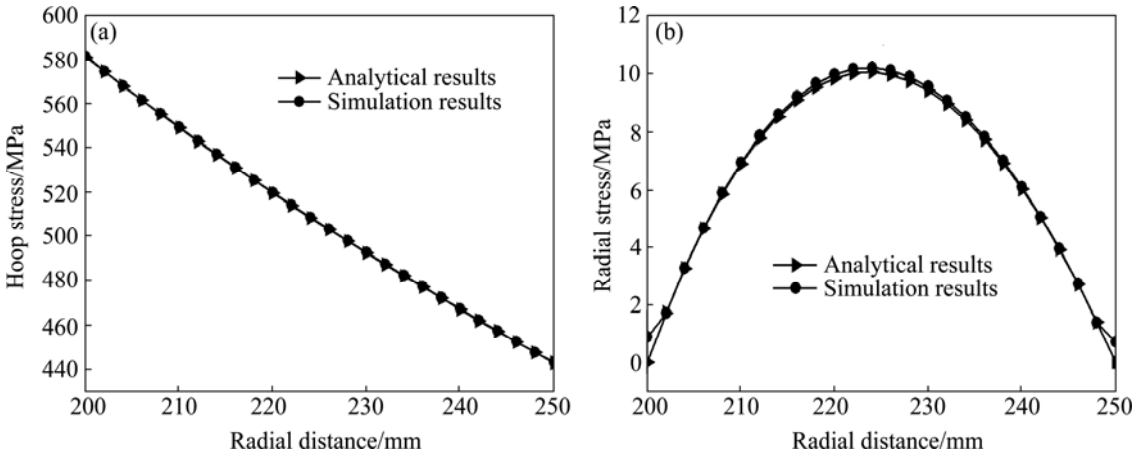

Fig. 3 Stress distributions of solid matrix ring: (a) Hoop stress; (b) Radial stress

value in the middle of the radial direction. The hoop stresses are much higher than the radial stresses for the 60th solid composite ring and solid matrix ring. Furthermore, comparing the stresses of the solid composite ring with that of the solid matrix ring, it is obviously revealed that the hoop stresses of the latter are higher, while the radial stresses are almost unchanged.

3.2 Stress analysis for TMCs ring at room temperature

Aeroengine compressor rotors at different levels work at different temperatures. It is well known that temperature has a significant effect not only on the thermal residual stresses, but also on the mechanical properties of the matrix cladding and composite core, so the stress distribution of the ring is analyzed at room temperature and 400 °C, respectively. Firstly, we discuss the stress distribution at room temperature under a rotating speed of 14320 r/min (hereafter all of the stress analysis is based on the same rotating speed). The stress distribution along radial, hoop, axial direction and von Mises stress of the ring with reinforced area 30 mm× 20 mm and 35% fiber volume fraction are shown in Fig. 4. The results show that the stresses in composite core along the radial and axial directions are compressive which are mainly induced by residual stresses. However, hoop stresses are tensile and have a maximum value at the ID of the ring. Comparing the stresses in all of the three directions, hoop stresses are much higher and play an important role on the deformation behavior of the ring, so all of the stress analyses below are based on the hoop direction at the path defined at y=0° and z=20, as a black arrow shown in Fig. 4(b). Figure 5 displays the hoop stresses distribution of the ring with reinforced area 30 mm×20 mm and 35% fiber volume fraction. It can be seen that the hoop stresses have a maximum value at the ID of the composite core and decrease gradually along the radial direction when the thermal residual stresses are not considered, while the hoop stresses have a peak value at the ID of the ring when considering thermal residual stresses. This is because when the TMCs ring is cooled after consolidation, the thermal residual stresses are generated due to the mismatch of CTEs between the matrix and the composite core. As the CTEs of the matrix are higher than thoes of the composite core, the matrix cladding goes into hoop tension and the

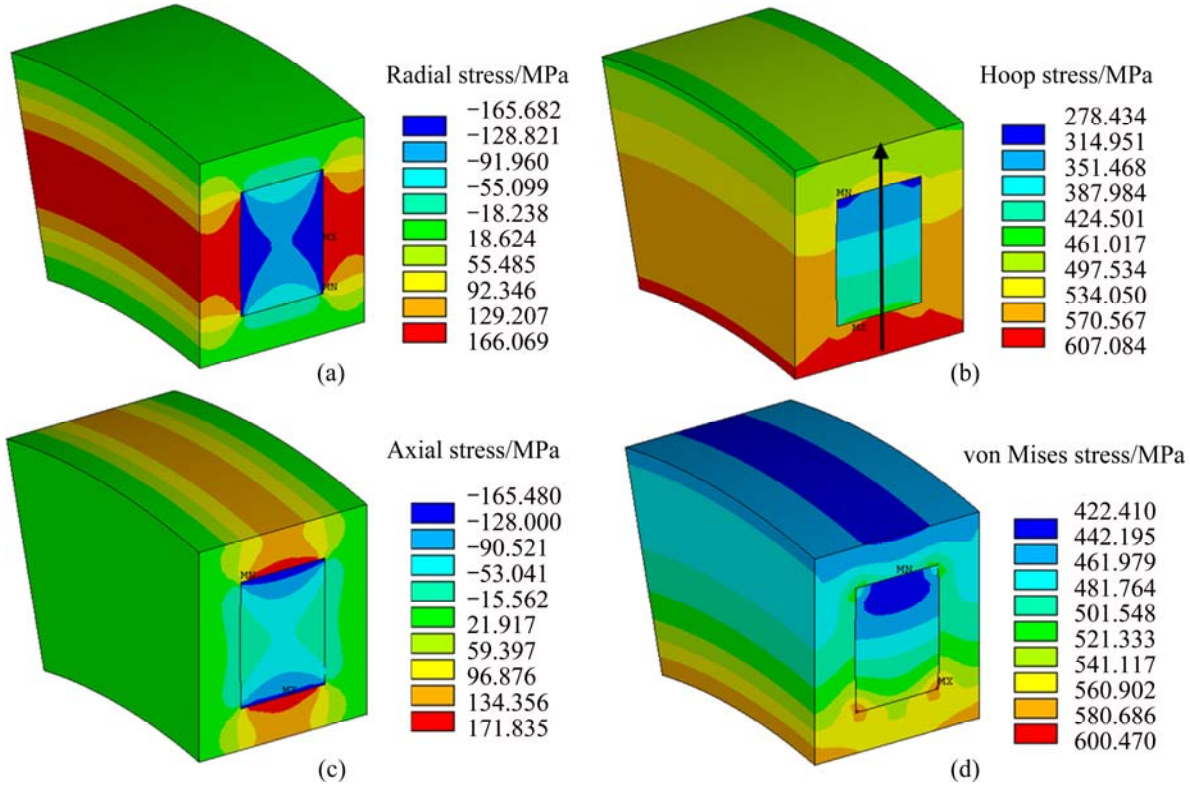

Fig. 4 Stress distributions of rings with residual stress at room temperature: (a) Radial direction; (b) Hoop direction; (c) Axial direction; (d) Von Mises stress

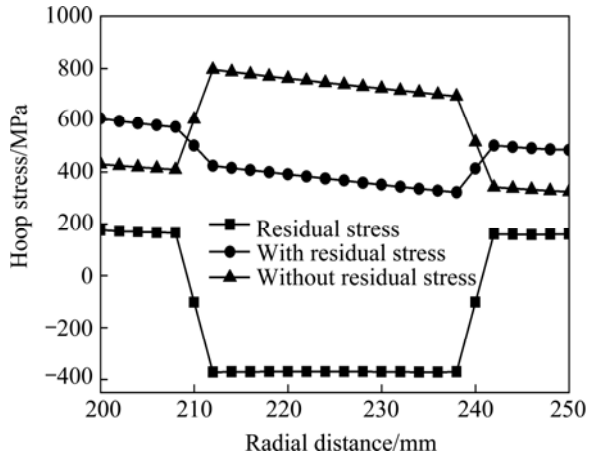

Fig. 5 Hoop stress distribution of TMC rings with reinforced area 30 mm×20 mm and 35% fiber volume fraction at room temperature

composite core goes into hoop compression. In addition, it can be found that the difference of the hoop stresses between including and excluding residual stresses is approximately equal to the value of residual stresses.

The hoop stress distribution of TMCs ring with different fiber volume fractions at room temperature are plotted in Fig. 6. According to Fig. 6(a), the residual stresses increase with increasing the fiber volume fraction. The reason is that the higher the fiber volume fraction, the lower the CTEs of the composite core, that is to say, the mismatch of the CTEs between the composite core and the matrix cladding is more obvious. From Fig. 6(c), it can be seen that with the increase of fiber volume fraction, the hoop stresses increase in the composite core, whereas decrease in the matrix cladding when the residual stresses are not considered. The reason is that the strength of the composites increases along the fiber direction as fiber volume fraction increases, so the composite core burdens more hoop stresses while the matrix cladding undertakes less. When considering residual stresses (see Fig. 6(b)), the maximum value of hoop stresses locates at the ID of the ring. Moreover, the higher the fiber volume fraction, the lower the hoop stresses in the composite core, and the hoop stresses in the matrix cladding are almost at the same level. This can be explained by the fact that the difference of residual stresses in the composite core among different fiber volume fractions is larger than that of hoop stresses when not considering the residual stresses. For instance, the compressive residual stresses in the composite core are approximately 370 MPa and 417 MPa for 35% and 40% fiber volume fractions, respectively, thus the difference is 47 MPa. However, the maximum value of hoop stresses at the ID of the composite core are 795 MPa and 820 MPa for 35% and 40% fiber volume fractions respectively without residual stresses, so the difference is only 25 MPa.

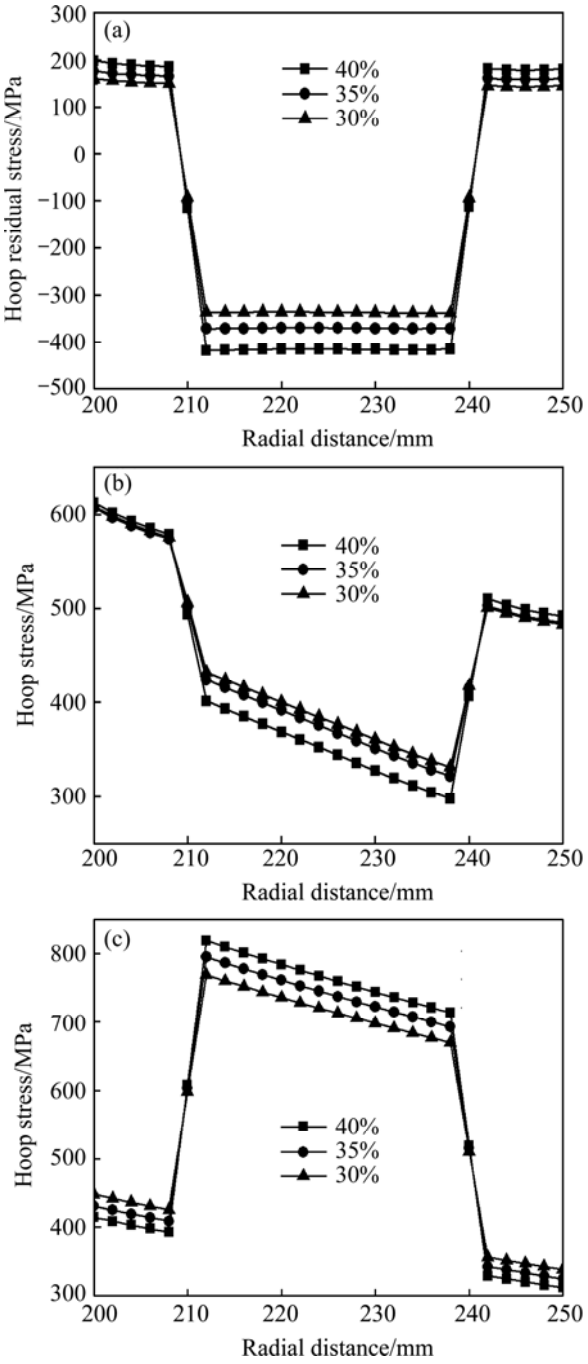

Fig. 6 Hoop stress distribution of TMC rings with different fiber volume fractions at room temperature: (a) Hoop residual stress; (b) With residual stress; (c) Without residual stress

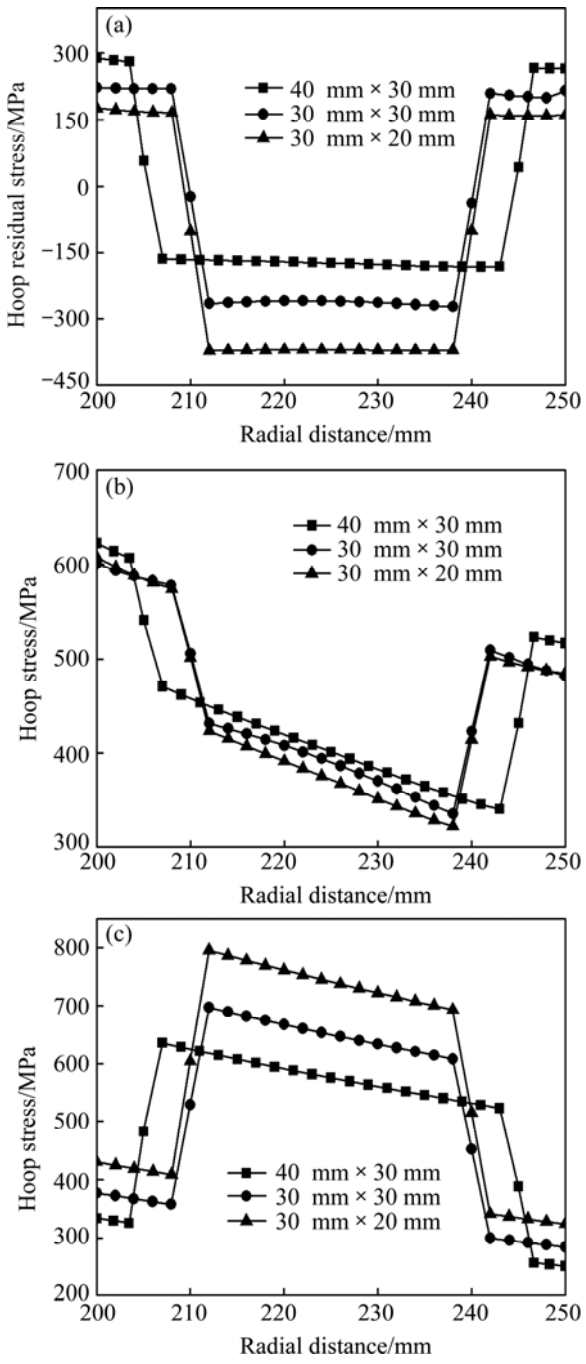

Fig. 7 Hoop stress distribution of TMC rings with different reinforced areas at room temperature: (a) Hoop residual stress; (b) With residual stress; (c) Without residual stress

The hoop stress distributions of TMC rings with different reinforced areas at room temperature are illustrated in Fig. 7. Figure 7(a) describes the distributions of hoop residual stresses with different reinforced areas. The results show that the compressive residual stresses in the composite core decrease with increasing the reinforced area. However, the tensile residual stresses in the matrix cladding decrease with decreasing the reinforced area. This can be comprehended by two limit cases. One case is that the ring is made of full composite (i.e., reinforced area reaches the maximum), then no CTEs mismatch between the matrix cladding and the composite core, thus no compressive residual stresses exist in the composite core. The other case is that the ring is composed of pure matrix (i.e., reinforced area reaches minimum), then the tensile residual stresses in matrix cladding do not exist. As shown in Fig. 7(c), the hoop stresses reduce overall with increasing the reinforced area when the residual stresses are not considered. The maximum hoop stresses at the ID

of the composite core are approximately 800 MPa and 630 MPa for reinforced area 30 mm×20 mm and 40 mm×30 mm, respectively. When the ring is fabricated with pure composites, the maximum hoop stress is even less than 500 MPa (see Fig. 3(a)). When the residual stresses are considered, the higher the reinforced area, the higher the hoop stresses (see Fig. 7(b)). The maximum values of hoop stresses in the composite core are 430 MPa and 470 MPa for reinforced area 30 mm× 20 mm and 40 mm×30 mm, respectively. This is because the gap of the compressive residual stresses among different reinforced areas is larger than that of hoop stresses without residual stresses. For example, the compressive residual stresses in the composite core are nearly 370 MPa and 165 MPa for reinforced area 30 mm×20 mm and 40 mm×30 mm, respectively, then the difference is 205 MPa, which is larger than that of the maximum hoop stresses (170 MPa) for the two different reinforced areas without residual stresses. From the above analyses, it can be drawn that at room temperature, relatively small reinforced area is beneficial to the ring, which may be contrary to our expectation.

3.3 Stress analysis for TMCs ring at 400 °C

The above analysis has presented the stress distributions of the TMCs ring at room temperature. However, the actual working temperature of TMCs ring is usually much higher than room temperature, so in this section, the stress distribution of the TMCs ring at 400 °C is analyzed. Figure 8(a) shows the hoop stress distributions of the ring with reinforced area of 30 mm×20 mm and 35% fiber volume fraction. The results show that the hoop stresses reach a maximum value at the ID of the composite core. This is different from the hoop stress distribution at room temperature with residual stresses in which the maximum hoop stresses locate at the ID of the ring. This can be attributed to the lower residual stresses. As discussed above, the matrix cladding is in hoop tension and the composite core is in hoop compression. Comparing the residual stresses at 400 °C with those at room temperature, it is obvious that the former is much lower than the latter. As shown in Fig. 8(c), at room temperature, the tensile residual stresses in the matrix cladding and the compressive residual stresses in composite core are approximately 170 MPa and 370 MPa, respectively. However, they decline to 60−70 MPa and 160 MPa at 400 °C due to the release of part of the residual stresses. In addition, the hoop stresses in the composite core at 400 °C are relatively higher than those at room temperature without the residual stresses (see Fig. 8(b)), while they are lower in the matrix cladding due to strength degradation of the matrix. It can be concluded that the difference of hoop stresses between the matrix

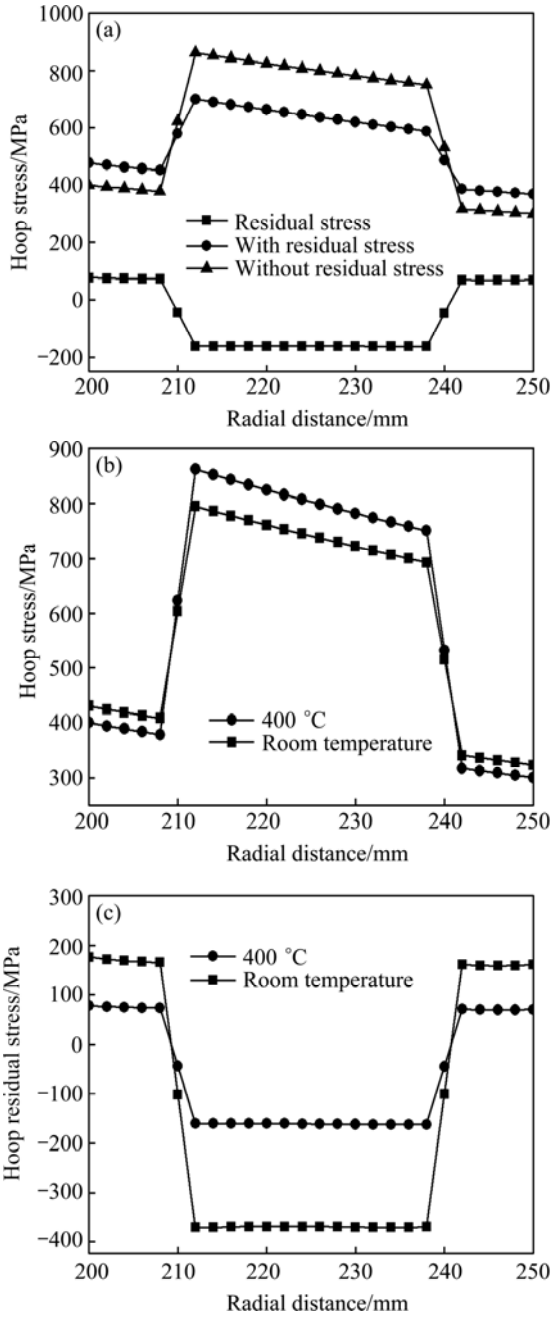

Fig. 8 Hoop stress distribution of TMC rings: (a) With/without residual stress and residual stress at 400 °C; (b) Without residual stress at room temperature and 400 °C; (c) Hoop residual stress at room temperature and 400 °C

cladding and composite core at high temperature is widening when not considering the residual stresses. This is also responsible for the fact that the hoop stresses have a maximum value at the ID of the composite core at 400 °C with the residual stresses.

Figure 9 demonstrates the hoop stresses distribution of TMC rings with different fiber volume fractions at 400 °C. It can be seen that the influence of fiber volume fraction on residual stresses is very similar to that at room temperature. With increasing the fiber volume

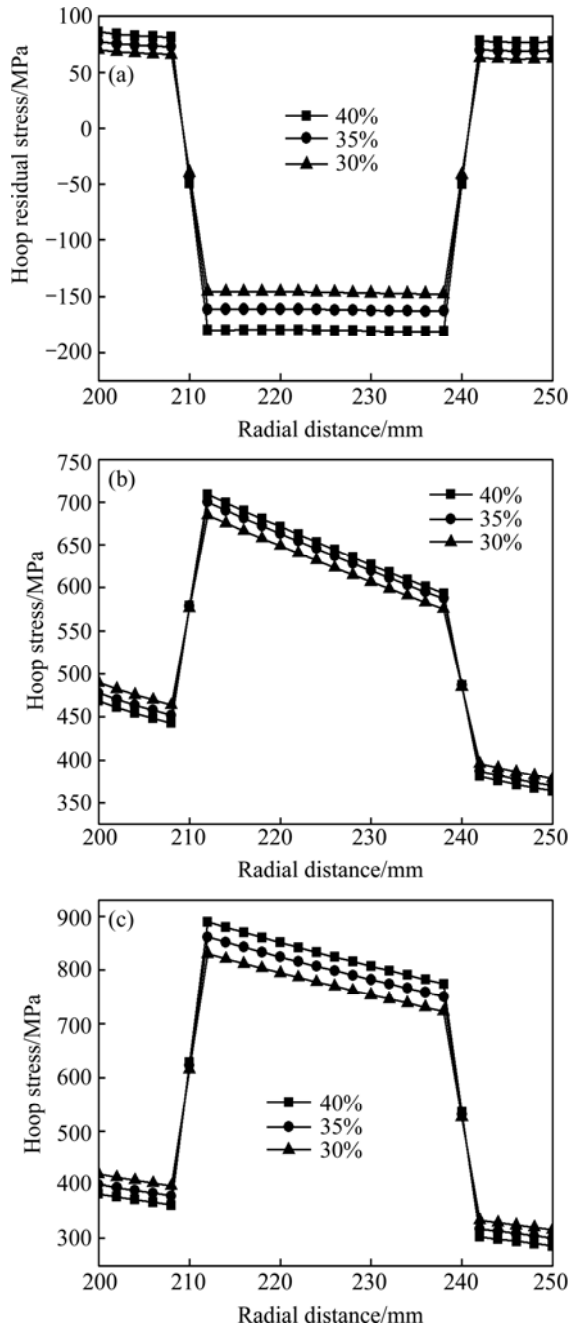

Fig. 9 Hoop stress distribution of TMC rings with different fiber volume fractions at 400 °C: (a) Hoop residual stress; (b) With residual stress; (c) Without residual stress

fraction, the residual stresses increase, though the values of residual stresses are much lower than those at room temperature. When the residual stresses are not considered (see Fig. 9(c)), the hoop stresses have a maximum value at the ID of the composite core. The maximum values of hoop stresses are 860 MPa and 890 MPa for 35% and 40% fiber volume fractions, respectively. The hoop stresses increase in the composite core, while decrease in the matrix cladding with increasing fiber volume fraction. This trend is similar to that at room temperature. However, when considering the residual stresses (see Fig. 9(b)), the trend has no changes (see Fig. 9(c)), merely the stress values are lower in the composite core due to the hoop compressive residual stresses and higher in the matrix cladding due to the hoop tensile residual stresses. The maximum hoop stresses locate at the ID of the composite core and the stresses in the composite core increase with increasing fiber volume fraction. This is mainly because the difference of residual stresses among different fiber volume fractions is lower than that of hoop stresses without residual stresses. For instance, the compressive residual stresses in composite core are approximately 160 MPa and 180 MPa for 35% and 40% fiber volume fractions, respectively, then the difference is 20 MPa, which is lower than that of the maximum hoop stresses (30 MPa) for the two fiber volume fractions without residual stresses.

Figure 10 displays the hoop stresses distribution of TMCs ring with different reinforced areas at 400 °C. It can be seen that the higher the reinforced area, the lower the overall hoop stresses, and the hoop stresses have a maximum value at the ID of the composite core whether considering the residual stresses or not. The maximum value of hoop stresses is approximately 660 MPa and 860 MPa for reinforced area 40 mm×30 mm and 30 mm×20 mm respectively when not considering residual stresses (see Fig. 10(c)), hence the difference is 200 MPa. Similar to the distribution of residual stresses with different reinforced areas at room temperature, the compressive residual stresses in the composite core decrease with increasing the reinforced area, while the tensile residual stress in the matrix cladding decreases with decreasing the reinforced area (see Fig. 10(a)). From Fig. 10(a), it also can be seen that the compressive residual stresses in the composite core is 70−80 MPa and 160 MPa for the reinforced areas 40 mm×30 mm and 30 mm×20 mm, respectively. The difference of residual stresses in the composite core between the two reinforced areas is 80−90 MPa, which is lower than that of the maximum hoop stresses for the two reinforced areas without residual stresses (200 MPa). Therefore, when considering the residual stresses, the value of hoop stresses is still the highest with the reinforced area 30 mm×20 mm. So it can be concluded that, at 400 °C, a larger reinforced area is beneficial.

3.4 Burst failure

In above analyses, the stress distributions are obtained under a constant rotating speed. However, with the increase of rotating speed, the hoop stresses would increase, therefore, when the rotating speed reaches a limit, the ring will burst failure. The burst speed of the TMCs ring, as the ultimate load capacity of the rotor component, is a key factor in design. So in this section,

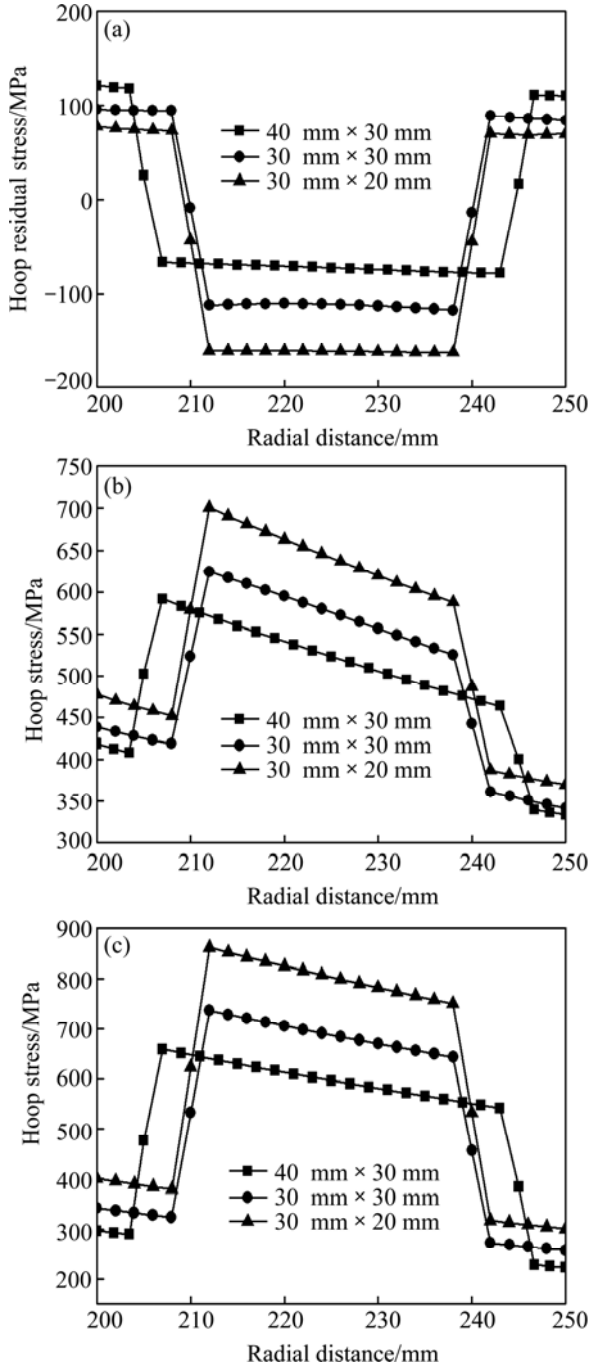

Fig. 10 Hoop stress distribution of TMC rings with different reinforced areas at 400 °C: (a) Hoop residual stress; (b) With residual stress; (c) Without residual stress

the burst speed is predicted from the perspective of security through analyzing the hoop tensile stress under a series of rotating speeds. According to Ref. [16], it was pointed out that the primary fracture surface after burst was caused by tensile overload of hoop direction, and the maximum hoop stresses numerically modeled at the burst speed was equivalent to 99.7% of the ultimate tensile strength of plate coupons. So as for the estimation of burst speed of TMC rings, the above "maximum hoop stress" criterion is used, that is, burst failure occurs at the instant that the maximum hoop stress exceeds the ultimate tensile strength of the composites in the fiber direction. Here, we only predict the burst speed of the ring reinforced with 30 mm×20 mm composite core with 35% fiber volume fraction at 400 °C. The longitudinal ultimate tensile strength of the composites at 400 °C has been calculated to be 1162 MPa in Section 2.2. As shown in Fig. 11(a), applying the "maximum hoop stress" criterion to the ID of the composite core where the maximum hoop stresses locate results in a burst speed of approximately 17200 r/min and 16520 r/min with and without residual stresses, respectively (in above analysis, the maximum stress of matrix cladding doesn't exceed its yield strength). So the compressive residual stresses in the composite core can offset part of hoop tensile stresses induced by centrifugal forces to avoid earlier failure of the TMC rings. However, the burst speed is much lower than that of a bling obtained through experiment test in Ref. [17], in which the burst speed was 55830 r/min. This is because the size of the bling is much smaller (the inner diameter is 140 mm and the outer diameter is 212 mm), so the centrifugal forces would be much lower at the same rotating speed. From Fig. 11(b), it is observed that the stress gradient between the ID and OD of the

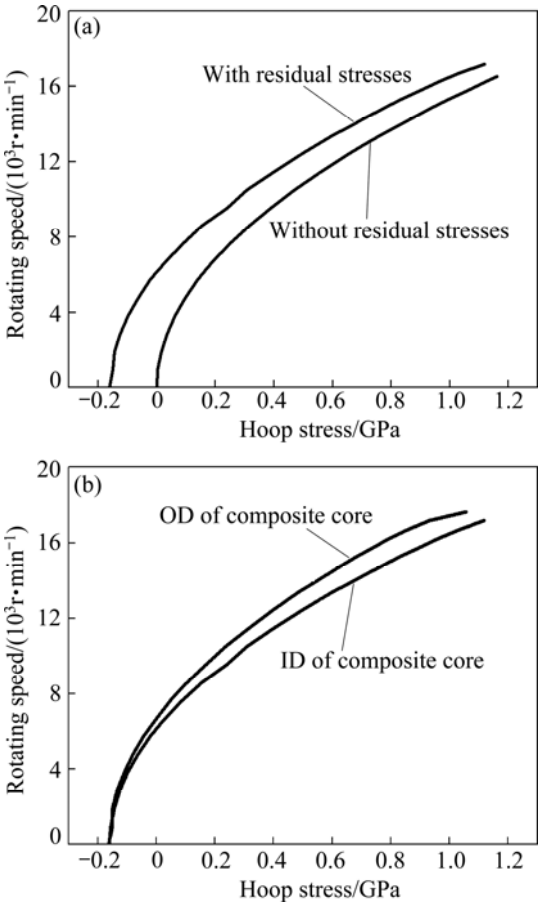

Fig. 11 Rotating speed vs hoop stresses at 400 °C: (a) At ID of composite core with/without residual stress; (b) At ID and OD of composite core with residual stress

composite core increases with increasing the rotating speed. The result is in accordance with the earlier literature [4].

4 Conclusions

1) The thermal residual stresses at room temperature are higher than those at 400 °C. When considering the thermal residual stresses, the maximum hoop stress at room temperature locates at the inner diameter of the ring, while it locates at the inner diameter of the composite core at 400 °C.

2) When considering thermal residual stresses, the hoop stresses in the composite core decrease with increasing fiber volume fraction, while that in the matrix cladding is almost the same at room temperature. However, the hoop stress in the composite core increases and that in the matrix cladding decreases respectively with increasing fiber volume fraction at 400 °C. The larger the reinforced area, the higher the hoop stresses at room temperature and the lower the hoop stresses at 400 °C.

3) The burst speeds of the TMCs ring are 17200 r/min and 16520 r/min with and without residual stresses, respectively.

References

[1] LEYENS C, KOCIAN F, HAUSMANN J, KAYSSER W A. Materials and design concepts for high performance compressor components [J]. Aerosp Sci Technol, 2003, 7(3): 201−210.

[2] LOU Ju-hong, YANG Yan-qing, SUN Qing. Study on longitudinal tensile properties of SiC_f/Ti−6Al−4V composites with different interfacial shear strength [J]. Mater Sci Eng A , 2011, 529: 88−93.

[3] CARRERE N, VALLE R, BRETHEAU T, CHABOCHE J L. Multiscale analysis of the transverse properties of Ti-based matrix composites reinforced by SiC fibres: From the grain scale to the macroscopic scale [J]. Int J Plast, 2004, 20(4): 783−810.

[4] ARNOLD S M, WILT T E. Deformation and life prediction of circumferentially reinforced SCS-6/Ti-15-3 ring, MMC life system development (Phase I)−A NASA/Pratt & Whitney life prediction cooperative program [R]. NASA RP-1361, 1996.

[5] ROBINSON D N, PASTOR M S. Limit pressure of a circumferentially reinforced SiC/Ti ring [J]. Compos Eng, 1992, 2(4): 229−38.

[6] NATSUMURA T, NOJIMA Y, SUZUMURA N, ARAKI T, MORIYA K, YASUHIRA K. Component design of CMC and MMC rotor for turbine engine applications [C]//Proceedings of the 31st International SAMPE Technical Conference, Chicago, 1999: 130−41.

[7] KRUCH S, CARRËRE N, CHABOCHE J L. Fatigue damage analysis of unidirectional metal matrix composites [J]. Int J Fatigue, 2006, 28(10): 1420−5.

[8] HILL R. The mathematical theory of plasticity [M]. London: Oxford University Press, 1998: 317−334.

[9] RILEY M B, WHITNEY J M. Elastic properties of fiber reinforced composite materials [J]. AIAA J, 1966, 4(9): 1537−1542.

[10] KARADENIZ Z H, KUMLUTAS D. A numerical study on the coefficients of thermal expansion of fiber reinforced composite materials [J]. Compos Struct, 2007, 78(1): 1−10.

[11] HUANG Bin. Study on the interface, microstructure and property of SiC_f/Ti composites [D]. Xi'an: Northwestern Polytechnical University, 2010. (in Chinese)

[12] FUKUSHIMA A, FUJIWARA C, KAGAWA Y, MASUDA C. Effect of interfacial properties on tensile strength in SiC/Ti–15–3 composites [J]. Mater Sci Eng A, 2000, 276(1): 243−249.

[13] LOU Ju-hong, YANG Yan-qing, LUO Xian, YUAN Mei-ni, FENG Guang-hai. The analysis on transverse tensile behavior of SiC/Ti−6Al−4V composites by finite element method [J]. Mater Design, 2010, 31(8): 3949−53.

[14] MA Zhi-jun, YANG Yan-qing, LÜ Xiang-hong, LUO Xian, CHEN Yan. The effect of matrix creep property on the consolidation process of SiC/Ti−6Al−4V composite [J]. Mater Sci Eng A, 2006, 433(1): 343−6.

[15] ARNOLD S M, SALEEB A F, AL-ZOUBI N R. Deformation and life analysis of composite flywheel disk systems [J]. Composites Part B, 2002, 33(6): 433−59.

[16] HONDA T, YUNOKI N, MORIYA K, NATSUMURA T, SUZUMURA N, UYAMA M. Experimental and analytical studies for cyclic spin of MMC rotor component [C]//Proceedings of the 32 nd International SAMPE Technical Conference, Boston, 2000: 650−660.

[17] MORIYA K, NOJIMA Y, NISHIDE S, YASUHIRA K. Fabrication of titanium metal matrix composite bring [C]//Proceedings of the 12th International Conference on Composite Materials (LCCML2). Paris, l999: ID415.

SiC_f/Ti−6Al−4V 复合材料叶环应力及超转失效的有限元分析

张红园，杨延清，罗 贤

西北工业大学 材料学院 凝固技术国家重点实验室，西安 710072

摘 要：建立钛基复合材料叶环三维循环对称有限元模型，分析其应力分布和超转失效。重点研究纤维体积分数、增强面积、热残余应力及 2 种不同温度对叶环应力分布的影响。通过分析在一系列转速下叶环的环向应力得到其极限转速。结果表明：在 2 种不同温度下，纤维体积分数和增强面积对叶环应力的分布和大小影响不同。研究结果为叶环的结构设计提供了一定的建议。当考虑热残余应力时，在较高的温度下，较大的增强面积对叶环的设计是有利的。

关键词：钛基复合材料；叶环；应力分布；超转失效；有限元模拟；热残余应力

(Edited by Yun-bin HE)